# Correction of $H_3^+$ Contributions in Hydrogen Isotope Ratio Monitoring Mass Spectrometry

**Alex L. Sessions,[†,‡] Thomas W. Burgoyne,[‡,§] and John M. Hayes*,[†]**

*Department of Geology and Geophysics, Woods Hole Oceanographic Institution, Woods Hole, Massachusetts 02543, and Biogeochemical Laboratories, Departments of Chemistry and of Geological Sciences, Indiana University, Bloomington, Indiana 47405*

**Two fundamentally different approaches, termed "pointwise" and "peakwise," are currently used to correct hydrogen isotope ratio monitoring data for the presence of $H_3^+$ ion contributions. Consideration of the underlying assumptions shows that the peakwise approach is valid only for peaks with the same functional shape and only when background signals do not vary. The pointwise correction is much more versatile and can be used even when peak shapes and sizes, as well as background signals, vary significantly. It is not exact and is limited in accuracy by (1) the signal-broadening effects of electronic time constants, (2) the analog-to-digital conversion frequency, and (3) the highest frequency of the sample signal. To minimize errors for typical gas chromatographic signals, time constants of <500 and analog-to-digital sampling intervals of ≤250 ms are needed. Errors are further minimized by matching sample and standard peaks in both amplitude and D/H ratio. Using the pointwise algorithm, we demonstrate that a series of 14 homologous $n$-alkanes varying in concentration over a 5-fold range can be analyzed with a mean precision of 2.3‰ and no systematic errors.**

Several methods have recently been described for measuring the $^2H/^1H$ (D/H) ratio of materials using isotope ratio monitoring mass spectrometry (irmMS). These methods utilize elemental analyzers[1] or gas chromatographs[2−5] to produce $H_2$ peaks in a continuous stream of carrier gas. Hydrogen in samples is converted to $H_2$ via pyrolysis or coupled oxidation/reduction and flows into an isotope ratio mass spectrometer. In all cases, mass-2 ($H_2$) and mass-3 (HD) ion beams are monitored continuously, and

D/H ratios are based on integration of the mass-2 and mass-3 ion current signals.

Data-processing procedures are similar to those used for carbon isotopic analyses: sample peaks and background signals are defined, peak areas are integrated and ratios are calculated, and δD values are obtained by comparing the D/H ratios of samples to those from reference peaks of known isotopic abundance.[6] For hydrogen isotopic analyses, however, the mass-3 ion current must be corrected for the presence of $H_3^+$ ions.[7]

Two basic approaches, termed "pointwise"[8] and "peakwise",[9] have been proposed to correct for the presence of $H_3^+$. While some successes have been reported with both of these approaches, neither has yet been shown to be universally applicable. To overcome such limitations, we report here a general method for processing hydrogen irmMS data, including the correction for $H_3^+$. This method can be used with all types of isotope ratio monitoring analytical systems, including elemental analyzers and gas chromatographs.

## THEORY

$H_3^+$ is formed in the ion source of the mass spectrometer by the reaction[7]

$$H_2^+ + H_2 \rightarrow H_3^+ + H^\bullet \tag{1}$$
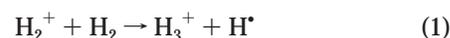
The abundance of $H_2^+$ is proportional to the partial pressure of $H_2$; hence, the production of $H_3^+$ is proportional to the second power of the partial pressure of $H_2$. In practice, it is convenient to substitute measured ion currents ($i$) for partial pressures, such that

$$i_{H_3} = K(i_{H_2})^2 \tag{2}$$

where $K$ is an experimentally determined proportionality constant.[7] The true isotope ratio of the sample (= D/H = $R^*/2$) is then

* Corresponding author: (email) JHayes@whoi.edu; (fax) 508-457-2183.

† Woods Hole Oceanographic Institution.

‡ Indiana University.

§ Present address: Department of Chemistry, Oklahoma State University, Stillwater, OK 74078.

(1) Kelly, S. D.; Parker, I. G.; Sharman, M.; Dennis, M. J. *J. Mass Spectrom.* **1998**, *33*, 735−738.

(2) Sessions, A. L.; Burgoyne, T. W.; Schimmelmann, A.; Hayes, J. M. *Org. Geochem.* **1999**, *30*, 1193−1200.

(3) Scrimgeour, C. M.; Begley, I. S.; Thomason, M. L. *Rapid Commun. Mass Spectrom.* **1999**, *13*, 271−274.

(4) Tobias, H. J.; Brenna, J. T. *Anal. Chem.* **1997**, *69*, 3148−3152.

(5) Hilkert, A. W.; Douthitt, C. B.; Schluter, H. J.; Brand, W. A. *Rapid Commun. Mass Spectrom.* **1999**, *13*, 1226−1230.

(6) Ricci, M. P.; Merritt, D. A.; Freeman, K. H.; Hayes, J. M. *Org. Geochem.* **1994**, *21*, 561−571.

(7) Friedman, I. *Geochim. Cosmochim. Acta* **1953**, *4*, 89−103.

(8) Tobias, H. J.; Goodman, K. J.; Blacken, C. E.; Brenna, J. T. *Anal. Chem.* **1995**, *67*, 2486-2492.

(9) Tobias, H. J.; Brenna, J. T. *Anal. Chem.* **1996**, *68*, 2281−2286.

**Table 1. Definition of Symbols and Typical Values of Instrumental Parameters**

| | |
|---|---|
| $i_2$ | total ion current at mass-2, ~5 nA |
| $i_{H_2}$ | ion current due to $H_2^+$, ~5 nA |
| $i_3$ | total ion current at mass-3, ~300 fA |
| $i_{H_3}$ | ion current due to $H_3^+$, ~40 fA |
| $i_{HD}$ | ion current due to $HD^+$, ~260 fA |
| $K$ | $H_3^+$ factor, ~20 ppm $mV^{-1}$ |
| $R$ | ratio of mass-3 to mass-2 ion currents |
| $R^*$ | $R$ corrected for $H_3^+$ contribution |
| $R^+$ | $R^*$ incorporating errors in $H_3^+$ correction |
| $P_{H_2}$ | partial pressure of $H_2$ in MS ion source, ~$10^{-7}$ mbar |
| $f(t)$ | any continuous function describing a peak-shaped curve |
| $A$ | integrated area under $f(t)$, A·s |
| $A_2$ | integrated area under $[f(t)]^2$, $A^2$·s |
| $c$ | proportionality constant relating $H$ and $A_2/A$ |
| $h$ | amplitude scaling factor in Gaussian-shaped peak |
| $\mu$ | mean value for Gaussian-shaped peak, s |
| $\sigma$ | standard deviation for Gaussian-shaped peak, s |
| $\delta D$ | isotopic composition of a sample relative to SMOW, ‰ |
| $\epsilon$ | relative error in integrated $i_{H_3}$, % |
| $\xi$ | error in calculated $\delta D$ value, ‰ |

calculated from

$$R = \frac{i_3}{i_2} = \frac{i_{HD} + i_{H_3}}{i_{H_2}} = \frac{i_{HD}}{i_{H_2}} + Ki_{H_2} = R^* + Ki_{H_2} \quad (3)$$

where $i_2$ and $i_3$ are the observed mass-2 and mass-3 ion currents and $R$ and $R^*$ represent the measured and corrected ion current ratios, respectively.

In hydrogen isotopic analyses, the proportionality constant $K$ is commonly referred to as the "$H_3$ factor" and is determined by measuring $R$ at multiple values of $i_2$ for a single sample. Equation 3 has the form $y = b + mx$, so that regression of $R$ on $i_2$ ($\approx i_{H_2}$) yields the value of $K$ as the slope of the regression. Typical units for $K$, which expresses a change in the $i_3/i_2$ ratio per unit increase in $i_2$, are $10^{-6}$ $mV^{-1}$ or $10^{-3}$ $nA^{-1}$. Under typical operating conditions, 5−30% of $i_3$ can be due to $H_3^+$. The correction for $H_3^+$ is therefore a significant one, and in "conventional" hydrogen isotopic analyses (i.e., repeated comparison of sample and reference gases introduced from dual viscous-leak inlets), it can be the limiting factor in the precision of the analyses.[10] It remains to be seen whether precision in irmMS techniques will also be limited by correction for $H_3^+$.

**$H_3^+$ Correction Algorithms.** Equation 3, as written, is strictly true only for instantaneous ion currents and is subject to the assumption that $i_{H_2}$ is proportional to $P_{H_2}$. In conventional analyses, isotope ratios are measured at constant $P_{H_2}$, so that *integrated* ion currents can be substituted for *instantaneous* ion currents. Small deviations in $i_2$ across an integration interval will produce little error in the correction for $H_3^+$ as long as variations are symmetrically distributed about the mean value.[10] In isotope ratio monitoring analyses, however, the partial pressure of $H_2$ in the ion source is changing rapidly and continuously as each sample peak passes through the mass spectrometer. Therefore, the ion current will often change significantly across a single 125-ms integration interval. Under these conditions, application of eq 3 is no longer straightforward.

(10) Schoeller, D. A.; Peterson, D. W.; Hayes, J. M. *Anal. Chem.* **1983**, *55*, 827−832.

Two strategies for $H_3^+$ correction of irmMS data have been proposed. Tobias et al.[8] first used a "pointwise" scheme in which, prior to peak integration, each measured value of $i_3$ was corrected based on the corresponding value of $i_2$. However, they observed a nonlinear dependence of $R$ on $i_2$, perhaps due to fractionation of hydrogen isotopes by the Pd membrane they used to eliminate He from the mass spectrometer. They later abandoned this approach in favor of a "peakwise" correction,[9] which was based on the amplitude of the chromatographic peak, rather than on individual measurements of $i_2$. The relationship between $R$ and peak height in the peakwise correction was also nonlinear. A similar approach was used by Scrimgeour et al.,[3] who also used a peakwise correction based on peak height, but who (in a system not including a Pd membrane) found a linear relationship between $R$ and peak height.

While these corrections have apparently been used successfully, there has not yet been any theoretical examination of their basis and characteristics. The first applications[1,3,8,9] investigated simple chromatograms with few analytes, constant peak shapes, and negligible chromatographic column bleed. It remains unclear whether the correction schemes can be applied accurately to peaks with different shapes, to partially coeluting peaks, to peaks superimposed on changing $H_2$ backgrounds, or under other conditions that are frequently encountered in the analysis of real samples.

**Peakwise Corrections.** For irmMS applications, the measured ratio of ion currents for any given peak is

$$R = \frac{\int i_3(t)\, dt}{\int i_2(t)\, dt} = \frac{\int i_{HD} + \int Ki_{H_2}^2}{\int i_{H_2}} = R^* + K\frac{\int i_{H_2}^2}{\int i_{H_2}} \quad (4)$$

where $i_2(t)$ and $i_3(t)$ are time-variable ion currents and each ion current is integrated with respect to time. We make the distinction between integrated ion currents in eq 4 and instantaneous ion currents in eq 3 to emphasize that ion currents are changing continuously in irmMS systems and that values of $i_2$ which have been averaged over some finite time *cannot* be used in eq 3.

From eq 4, any property of an integrated peak that is functionally related to the quantity $\int i_{H_2}^2 / \int i_{H_2}$ could in theory be used as the basis for a peakwise correction (i.e., to establish a useful relationship between $R$ and $R^*$). To explore this idea, we first examine the relationship between peak height and integrated areas in peaks having a Gaussian shape. Any such peak can be described by

$$f(t) = h \exp\left[-\frac{1}{2}\left(\frac{t - \mu}{\sigma}\right)^2\right] \quad (5)$$

where $\mu$ is the mean value, $\sigma$ is the standard deviation, and $h$ is an amplitude scaling factor. The overall height (amplitude) of a Gaussian peak is simply $h$, and the areas under $f(t)$ and $[f(t)]^2$ are

$$A \equiv \int_{-\infty}^{\infty} f(t)\, dt = h\sigma\sqrt{2\pi} \quad (6)$$

$$A_2 \equiv \int_{-\infty}^{\infty} [f(t)]^2\, dt = h^2\sigma\sqrt{\pi} \quad (7)$$

**Table 2. Heights and Integrated Areas for Several Peak-Shape Functions**

| defining function | peak height | $A^a$ | $A_2{}^a$ | $c^a$ |
|---|---|---|---|---|
| Gaussian $\quad f(t) = h\exp[-\frac{1}{2}(t/\sigma)^2],\ -\infty \le t \le \infty$ | $h$ | $h\sigma\sqrt{2\pi}$ | $h^2\sigma\sqrt{\pi}$ | $\sqrt{2}$ |
| rectangle $\quad f(t) = h,\ 0 \le t \le w$ | $h$ | $hw$ | $h^2 w$ | $1$ |
| triangle[b] $\quad f(t) = -mt + h,\ 0 \le t \le h/m$ | $h$ | $h^2/m$ | $5h^3/3m$ | $5/3$ |
| parabola $\quad f(t) = -at^2 + h,\ -\sqrt{\dfrac{h}{a}} \le t \sqrt{\dfrac{h}{a}}$ | $h$ | $\dfrac{4}{3}h\sqrt{\dfrac{h}{a}}$ | $\dfrac{11}{15}h^2\sqrt{\dfrac{h}{a}}$ | $20/11$ |
| Lorentzian $\quad f(t) = \dfrac{h(\Gamma/2)}{(t - \mu)^2 + (\Gamma/2)^2},\ -\infty \le t \le \infty$ | $2h/\Gamma$ | $h\pi$ | $h^2\pi/\Gamma$ | $2$ |
| sine $\quad f(t) = h\sin(t),\ 0 \le t \le \pi$ | $h$ | $2h$ | $h^2\pi/2$ | $4/\pi$ |

[a] See text for definitions. [b] Given function is for half of a triangle. Values for $A$, $A_2$, and $c$ are for the full (symmetric) triangle.

Comparing integrated peak areas (eqs 6 and 7) gives

$$\frac{A_2}{A} = \frac{h^2\sigma\sqrt{\pi}}{h\sigma\sqrt{2\pi}} = \frac{h}{\sqrt{2}} \tag{8}$$

Since $A_2/A$ is analogous to $\int i_{H_2}^2 / \int i_{H_2}$, eq 8 shows that the peak height of any Gaussian-shaped chromatographic peak is directly proportional to $\int i_{H_2}^2 / \int i_{H_2}$ regardless of the size or width of the peak.

Values for $c$, a proportionality constant relating peak height and $A_2/A$, are tabulated for several other functions in Table 2. While each function has a characteristic value of $c$, these vary significantly between functions so that no single, peakwise calibration could be used to compare peaks with different functional shapes. For example, Gaussian peaks cannot be compared with rectangular reference peaks. This is in agreement with the observation of Tobias and Brenna[9] that the peakwise correction is dependent on constancy of peak shape.

Further complications arise when background $H_2$ currents are present. The abundance of $H_3^+$ is proportional to the second power of the entire $H_2$ ion current, and contributions from sample $H_2$ and background $H_2$ cannot be added linearly. Stated mathematically,

$$i_{H_3} = K(i_{H_2(samp)} + i_{H_2(bkgnd)})^2 \ne K i_{H_2(samp)}^2 + K i_{H_2(bkgnd)}^2 \tag{9}$$

Accordingly, correction for contributions of $H_3^+$ must take place *before* subtraction of background ion currents due to $H_2$. In cases where background currents change substantially, a straightforward application of the peakwise correction will not be possible.

**Pointwise Corrections.** The pointwise algorithm represents a fundamentally different approach to $H_3^+$ correction.[8] In essence, the instantaneous ion currents required by eq 3 are approximated by integrating ion currents over very short intervals. Errors result when ion currents change significantly during a single measurement interval, and the precision of the pointwise correction is therefore limited in part by the frequency at which ion currents are digitized. On the other hand, the only data needed to compute a pointwise correction are the values of $K$, $i_2$, and $i_3$. The size and shape of the peaks, and the separation of sample and background components, do not influence the correction.

In practice, the pointwise algorithm is implemented by correcting each measurement of $i_3$ based on the $i_2$ measurement from the same time interval using the equation $i_{HD} = i_3 - K(i_{H_2})^2$. The value for $K$ used in this equation should, to the extent possible, represent only the effects of $H_3^+$ formation on the measured ratio. Incorporation of other mass discrimination effects, such as those originating in inlet systems, the mass spectrometer, etc., is theoretically possible (for example, see ref 8), but the correction becomes increasingly nonlinear and instrument-specific. The equations and error analysis developed here are not applicable to a nonlinear $H_3^+$ correction. With only the effects of $H_3^+$ formation accounted for by $K$, the pointwise $H_3^+$ correction can be applied to virtually any hydrogen irmMS system. In an accompanying paper (Sessions et al., following paper), we describe several methods for measuring values of $K$ and show that the value obtained for pointwise correction of irmGCMS data is approximately the same as that used for conventional analyses.

To summarize, the peakwise approach to $H_3^+$ correction does have a firm theoretical basis. Provided that peak shapes and background $H_2$ currents are constant, the peakwise correction is exact and can succeed.[3,4,9,11] However, the required consistent peak shapes and background signals are seldom encountered in isotope ratio monitoring experiments and the potential for significant errors is great. In contrast, the pointwise approach to $H_3^+$ correction is approximate in all cases but is not significantly influenced by changes in peak shape or background signals. This flexibility provides a significant advantage over the peakwise approach, provided that the approximation embodied in the pointwise correction (i.e., that ion currents are constant over each integration interval) is sufficiently accurate. Below, we examine quantitatively the sources of error in the pointwise correction and show that for most isotope ratio monitoring measurements the error introduced by this method should not be precision-limiting.

## EXPERIMENTAL SECTION

Hydrogen isotopic compositions of *n*-alkanes were measured using a conventional GC coupled to an isotope ratio mass

(11) Tobias, H. J.; Brenna, J. T. *Anal. Chem.* **1996**, *68*, 3002−3007.

spectrometer via a 1400 °C pyrolysis furnace. The flow of He carrier gas into the mass spectrometer was 200 $\mu L/min$ and an electrostatic lens was used to prevent scattered $^4He^+$ ions from reaching the mass-3 detector. Details of this analytical system are provided in Sessions et al. (following paper).

**Samples.** A standard solution containing a homologous series of 15 n-alkanes (from n-$C_{16}$ to n-$C_{30}$) was prepared and used to test $H_3^+$ correction algorithms. The $\delta D$ values of the individual alkanes, which ranged from $-42$ to $-256$‰, were determined by Dr. Arndt Schimmelmann at Indiana University following the method described by Schimmelmann et al.[12] As recommended by Coplen,[13] the results of the off-line analyses were normalized to yield $\delta D$ (SLAP) = $-428$‰. Concentrations of the compounds in the standard solution yielded between 20 and 100 nmol of $H_2$/$\mu L$ and were chosen so that they did not correlate with either carbon number or hydrogen isotopic composition. $\delta D$ measurements for the first analyte in each chromatogram (n-$C_{16}$) were found to be significantly less precise ($\sigma = 10$‰) than for subsequent peaks ($2.1 \leq \sigma \leq 5.2$‰) and were excluded from all subsequent calculations. We have no precise explanation for this "first-peak" effect.

**Data Processing.** Ion currents at masses-2 and -3 were digitized and recorded at intervals of 62, 125, or 250 ms using Isodat v7.2−00 software (Finnigan MAT, Bremen, Germany). Raw ion current measurements and times were transferred into Excel (Microsoft, Redmond, WA), and further data processing was managed by Visual Basic codes that we have developed. These codes are available at http://www.nosams.whoi.edu/jmh. First, background ion currents not related to $H_2$ are subtracted. Components include offset currents added to each signal to provide a more stable background ratio[14] as well as contributions from $^3He^+$, $^4He^{2+}$, and scattered $^4He^+$ ions. Next, the data stream is corrected for the presence of $H_3^+$ on a point-by-point basis using the equation $i_{HD} = i_3 - i_{H_3} = i_3 - K(i_{H_2})^2$. Peaks are then identified and defined by examining the first and second derivatives of the $i_2$ signal over ~1-s intervals. Typically, slopes of 1.0 and $-0.1$ mV/s are used to define the beginning and end of the peak, respectively.

Next, the difference in time between the maxima of the $H_2$ and HD peaks is calculated as described—for the case of $^{12}CO_2$ and $^{13}CO_2$—by Ricci et al.[6] As with carbon isotopic measurements, this difference results from partial chromatographic separation of isotopically substituted molecules. For hydrogen isotopic measurements, the differences in retention time (for peaks containing a natural abundance of D) can be as large as 1 s, compared to ~100 ms for typical separations between carbon isotopic peaks. The data-processing algorithms used in this work adjust the peak start and stop times for the mass-2 and -3 peaks by whole numbers of data points (i.e., increments of 62, 125, or 250 ms) so that equivalent portions of each peak are integrated.

Background ion currents (including $H_2$-related components) for the n-alkane standard described above are assumed to be constant across the width of each peak and are determined by averaging $i_2$ and $i_3$ across 5-s intervals prior to each peak. Background currents for masses-2 and -3 in this system are typically 40 pA and 50 fA, respectively, with the GC column at 50
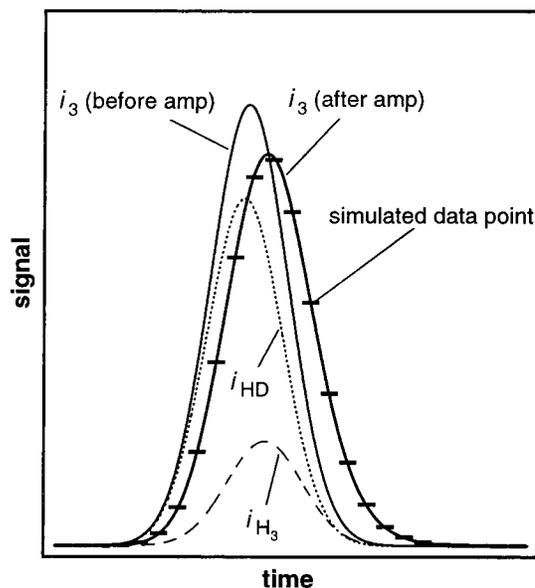
(12) Schimmelmann, A.; Lewan, M. D.; Wintsch, R. P. *Geochim. Cosmochim. Acta* **1999**, *63*, 3751−3766.

(13) Coplen, T. B. *Chem. Geol.* **1988**, *72*, 293−297.

(14) Merritt, D. A.; Hayes, J. M. *Anal. Chem.* **1994**, *66*, 2336−2347.

**Figure 1.** Typical output from the simulation of a Gaussian peak. $H_3^+$ and HD peaks are offset due to isotope chromatography. The sample peak is broadened by the existence of a 1.3-s time constant in the signal amplification circuit.

°C and 200 pA and 133 fA at 320 °C. Finally, peak areas are integrated, isotope ratios are calculated, and values of $\delta D$ are calculated by reference to standards.[13]

No organic standards are currently available with $\delta D$ near that of SLAP ($-428$‰). We therefore calibrated the irmGCMS data relative to the dual-inlet values to produce the desired normalization to the SMOW-SLAP scale, as follows. For each n-alkane analysis, the slope and intercept of the regression of irmGCMS $\delta D$ values on dual-inlet $\delta D$ values was calculated. As will be shown, this consistently yields a linear relationship with $r^2 > 0.99$. The average slope and intercept of all n-alkane analyses for a given day were then taken as the normalization line which was applied to all analyses on that day.

**Estimation of Errors and Uncertainties.** To test the sensitivity of results to errors introduced during data collection and processing, we constructed a numerical simulation that describes all ion currents produced during measurement of a sample peak. These include $H_2^+$, $HD^+$, and $H_3^+$ produced by both sample and background components, plus non-hydrogen background at masses 2 and 3. The simulation allows the use of different functions to define peak shape, including rectangular and Gaussian peaks of variable size. The effects of amplifier time constants are also calculated.[15] The resulting model data are then "digitized" at any desired frequency to produce a stream of simulated $i_2$ and $i_3$ data points, which mimics the actual data obtained from the mass spectrometer (Figure 1).

These simulated data, for which the accurate D/H ratios are known, can then be processed using various peak definition and $H_3^+$ correction algorithms. Comparison of the D/H ratios obtained to the true ratios then provides a quantitative estimate of error. This approach supplements the direct observation of results from test samples by separating and quantifying the individual effects

(15) Sternberg, J. C. In *Advances in Chromatography*; Giddings, J. C., Keller, R. A., Eds.; Dekker: New York, 1966; Vol. 2, pp 205−270.

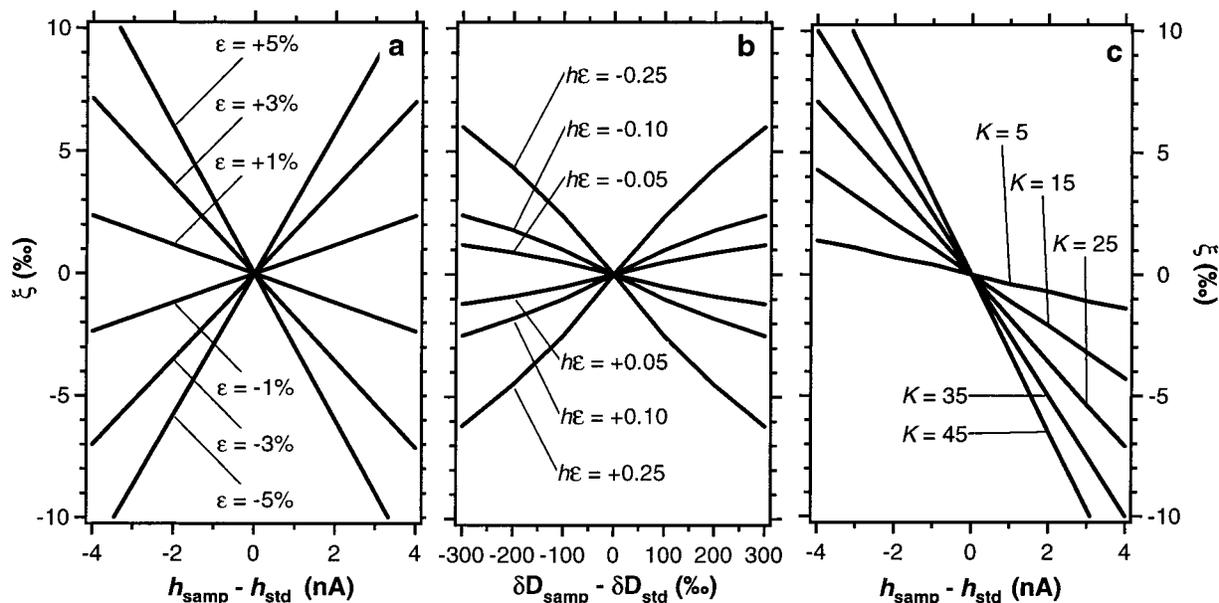**Figure 2.** Errors in $\delta D$ ($\equiv \xi$) as a function of pertinent variables: (a) as a function of error in integrated $i_{H_3}$ ($\equiv \epsilon$) and mismatched peak height ($h$) with matched $\delta D$ values and with $K = 25$; (b) as a function of $\epsilon$ and mismatched $\delta D$ values with matched peak heights and $K = 25$; (c) as a function of $K$ and mismatched peak heights with matched $\delta D$ values and $\epsilon = 1\%$. Units for $h$ are nA, and for $K$ are ppm mV$^{-1}$.

of frequency response, analog-to-digital conversion, and $H_3^+$ correction on the overall analytical uncertainty.

## RESULTS AND DISCUSSION

**Propagation of Errors.** Errors in $H_3^+$ correction will cause errors in calculated values of $\delta D$. The magnitude of the errors in $\delta D$ will depend on (1) the mismatch in size between sample and standard peaks, (2) the magnitude of $K$, and (3) the difference in D/H ratio of the sample and standard. To consider these factors both efficiently and quantitatively, we examine errors in $\delta D$ as a function of the relative error in $K$. Relative errors in $K$ and $H_3^+$ are equal, so that a 5% error in $K$ will cause a 5% error in the magnitude of the integrated $H_3^+$ ion current. Below we report errors in integrated $H_3^+$ due to signal collection and processing (i.e., which are not due to errors in the value of $K$). In a companion paper (Sessions et al., following paper), we report errors in the value of $K$ obtained by several methods. Both sources of error are readily incorporated in the analysis provided here.

As a representative example, we consider the comparison of a sample−standard pair of Gaussian-shaped peaks. The $\delta D$ value of a sample peak is calculated relative to the isotopic ratio of standard mean ocean water (SMOW) from

$$\delta D_{samp} = \left[ \frac{R^*_{samp}}{R^*_{SMOW}} - 1 \right] \times 1000 \qquad (10)$$

where $R^*$ is the $H_3$-corrected HD/$H_2$ ratio. Since the isotopic standard in use rarely has an HD/$H_2$ ratio equal to that of SMOW, eq 10 can be modified for use with a standard peak having any $\delta D$ value

$$\delta D_{samp} = \left[ \frac{R^*_{samp}}{R^*_{std}} \left( \frac{\delta D_{std}}{1000} + 1 \right) - 1 \right] \times 1000 \qquad (11)$$

For any Gaussian function, the value of $R^*$ can be obtained by combining eqs 4 and 8 to give

$$R^* = R - K \frac{\int i_2^2}{\int i_2} = R - K \frac{h}{\sqrt{2}} \qquad (12)$$

where $h$ is the height of the peak. If $K$ has a relative error $\epsilon$, the resulting, erroneously corrected HD/$H_2$ ratio of the peak becomes

$$R^+ = R - (K + \epsilon K) \frac{\int i_2^2}{\int i_2} = R - (1 + \epsilon) K \frac{h}{\sqrt{2}} \qquad (13)$$

The resulting error in $\delta D$, $\xi$, will then be given by

$$\xi = \delta D_{meas} - \delta D_{true} = (\delta D_{std} + 1000) \left[ \frac{R^+_{samp}}{R^+_{std}} - \frac{R^*_{samp}}{R^*_{std}} \right] \qquad (14)$$

Values of $R^*$ and $R^+$ can be evaluated directly from eqs 12 and 13. The error in $\delta D$ can, therefore, be determined using representative values of $\epsilon$, $K$, $R$, and $h$ for both sample and standard peaks (this approach assumes the magnitude of $\epsilon$ is identical in both sample and standard peaks). Values of $K$, $R$, and $h$ are readily obtained from experimental data.

Typical relationships obtained from eq 14 are illustrated in Figure 2. In the first instance, we consider errors in $\delta D$ when the $\delta D$ values of the sample and standard are approximately matched. To a good approximation, values of $\xi$ then depend only on the difference in peak height between sample and standard and on the magnitude of $\epsilon$ (Figure 2a). If sample and standard peaks are perfectly matched in height but not $\delta D$ value, $\xi$ varies approximately with the difference in $\delta D$ and with the product of $h$
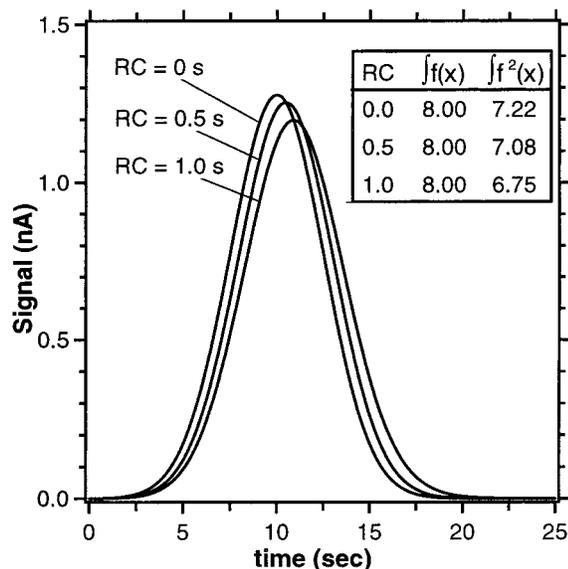
**Figure 3.** Decrease in the area under the square of signal intensity when peak shape is broadened by electronic time constants. All three curves represent the same 10-s-wide Gaussian curve filtered by three different time constants. This decrease in the ratio of integrated areas leads to an underestimate of $H_3^+$ contributions.



**Figure 4.** Estimated values of $\epsilon$ as a function of peak width and mass-2 time constant. Data are for Gaussian (solid lines; $\sigma$ = standard deviation) and rectangular (dashed lines; w = width) peaks with no background $H_2$ signals.

and $\epsilon$ (Figure 2b). In this case, errors increase with peak height (as opposed to the *difference* in peak heights) and with increasing mismatch in $\delta D$ values. In the third instance, errors in $\delta D$ increase as the magnitude of $K$ increases (Figure 2c) regardless of mismatch in peak height between sample and standard. Given the relationships in Figure 2, steps to minimize $H_3$-related errors in hydrogen irmMS analyses should be, in order of importance, (1) match sample and standard peak heights, (2) reduce the magnitude of $K$, (3) match sample and standard $\delta D$ values, and (4) with due attention to limitations imposed by shot noise,[14] minimize peak heights. This final step is counterintuitive, but is a result of the fact that $H_3^+$ increases disproportionately with increasing $H_2$.

**Detector Frequency Response.** Equations 2−4 assume that the mass-2 signal recorded by the data system accurately reflects the partial pressure of $H_2$ in the ion source. In fact, the relationship is only approximate. The mass-2 ion current follows $P_{H_2}$, but the signal voltage is affected by time constants associated with the signal-processing pathway. Although the time constant of the mass-2 amplifier could easily be <1 ms, an important requirement is that the time constants of both mass-2 and -3 amplifiers be approximately equal for greatest measurement accuracy.[14] Because of the large feedback resistance typical of the mass-3 amplifier ($\sim10^{12}$ $\Omega$), it is difficult to reduce time constants in that circuit below $\sim$500 ms.

If the time constant associated with the mass-2 signal pathway is so large, or if the chromatographic peaks are so narrow that their shape is not accurately reproduced by the signal-processing system, large errors in the calculated $H_3^+$ peak area, and so also the D/H ratio, will result. The nature of this problem is illustrated in Figure 3. As the time constant becomes larger, the signal peak is progressively broadened. Although the integrated area under $f(t)$ remains constant despite this broadening, the area under $[f(t)]^2$ does not. Instead, the integral of $[f(t)]^2$ decreases as the
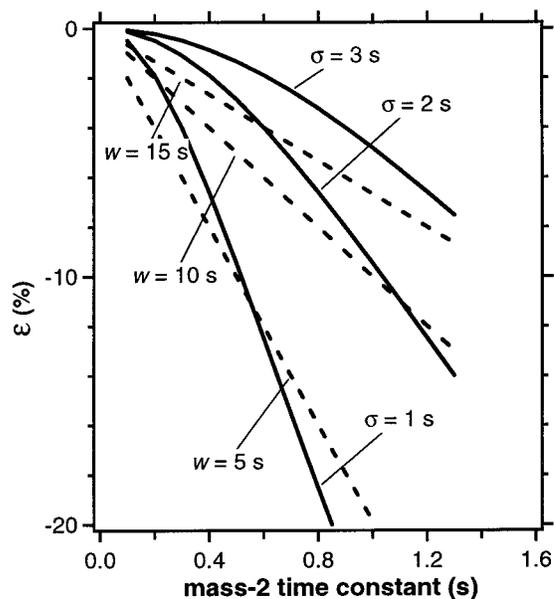
signal is broadened, resulting in underestimation of the $H_3^+$ contribution to $i_3$.

To examine the importance of frequency response quantitatively, we have calculated values of $\epsilon$ as a function of the time constant of the mass-2 signal pathway. Results are shown in Figure 4 for both Gaussian and rectangular peaks. The plotted results reflect calculations that consider only the effects of frequency response. As shown in Figure 4, errors related to the analog time constants increase sharply with decreasing peak width and increasing time constant and can be quite large. For Gaussian peaks with $\sigma$ = 3 s, an amplifier time constant of 1 s results in a value for $\epsilon$ of approximately −5%, and a time constant of 500 ms results in a value for $\epsilon$ of about −1%. These values of $\epsilon$ can be used directly in Figure 2 to estimate the magnitude of errors in $\delta D$. Note that in all cases the contribution of $H_3^+$ is underestimated. There are thus very clear benefits to maximizing the frequency response of both mass-2 and -3 detectors for hydrogen irmMS. Time constants of 500 ms or less should probably be considered a minimum requirement for chromatographic peaks with width ($4\sigma$) $\approx$ 10 s.

**Analog-to-Digital Conversion Rate.** Errors will be introduced by the pointwise $H_3^+$ correction when signals change significantly across individual integration intervals. The magnitude of the errors will depend on how fast signals are changing relative to the sampling rate. Numerical simulations confirm that $\epsilon$ decreases with sampling rate and increases as peaks get taller and narrower (Figure 5). For peaks having a width ($4\sigma$) of >4 s, an integration interval of 250 ms results in 0.0% $\geq$ $\epsilon$ $\geq$ −0.3%. Again, the contribution of $H_3^+$ to $i_3$ is underestimated. For square peaks, errors are negligible because ion currents are approximately constant over most of the peak.

**Sample Analyses.** As a test of the overall analytical system, including data-processing algorithms, the *n*-alkane test solution was analyzed 48 times over a period of 30 days. For these analyses, time constants of 0.2 (mass 2) and 1.3 s (mass 3) were used.

## Table 3. Peak Characteristics and δD Values of *n*-Alkane Standard

| C no. | $H_2$ (nM)[a] | $H$ (V)[b] | fwhm (s)[c] | δD (‰)[d] | $\sigma_{di}$ (‰)[e] | Δ (‰)[f] | $\sigma_p$ (‰)[e] | $\sigma_m$ (‰)[e] | $\sigma_\Delta$ (‰)[e] |
|---|---|---|---|---|---|---|---|---|---|
| 17 | 20.7 | 1.6 | 3.4 | −144.3 | 0.40 | 0.3 | 5.2 | 0.74 | 0.8 |
| 18 | 31.4 | 2.5 | 3.8 | −55.2 | 0.69 | ≡0[g] | | | |
| 19 | 41.9 | 3.6 | 4.0 | −119.4 | 0.92 | −2.6 | 3.2 | 0.47 | 1.0 |
| 20 | 52.2 | 5.1 | 4.5 | −48.7 | 0.40 | 1.8 | 2.7 | 0.39 | 0.6 |
| 21 | 10.2 | 1.2 | 4.1 | −215.0 | 1.21 | 2.3 | 3.8 | 0.56 | 1.3 |
| 22 | 20.9 | 2.2 | 4.0 | −62.2 | 0.75 | 3.0 | 2.3 | 0.33 | 0.8 |
| 23 | 31.3 | 3.4 | 4.0 | −46.5 | 1.21 | 1.1 | 2.1 | 0.31 | 1.3 |
| 24 | 42.0 | 4.7 | 4.3 | −55.4 | 1.10 | 3.8 | 2.7 | 0.40 | 1.2 |
| 25 | 52.1 | 5.8 | 5.0 | −256.5 | 1.39 | −1.4 | 2.2 | 0.32 | 1.4 |
| 26 | 10.4 | 1.4 | 4.5 | −57.7 | 0.64 | −4.5 | 4.1 | 0.59 | 0.9 |
| 27 | 20.7 | 2.6 | 4.5 | −226.5 | 0.98 | −0.6 | 3.6 | 0.52 | 1.1 |
| 28 | 31.2 | 3.8 | 5.1 | −52.3 | 0.92 | ≡0[g] | | | |
| 29 | 41.6 | 4.3 | 6.3 | −182.1 | 0.06 | 1.1 | 2.6 | 0.37 | 0.4 |
| 30 | 51.7 | 4.6 | 7.9 | −42.7 | 0.58 | −3.1 | 3.0 | 0.44 | 0.7 |
| mean | | | | | | 0.0 | 2.3 | | 1.0 |

[a] Injected on-column for typical analysis. [b] Peak height for typical analysis. [c] Full width at half-maximum for typical analysis. [d] Mean δD value from offline dual-inlet measurements ($n = 3$). [e] Standard deviations of the mean dual-inlet δD value ($\sigma_{di}$), the population of irmMS δD measurements ($\sigma_p$), the mean irmMS δD measurements ($\sigma_m$), and Δ ($\sigma_\Delta$). [f] $\Delta \equiv \delta D_{irmMS} - \delta D_{di}$. [g] *n*-$C_{20}$ and *n*-$C_{28}$ were the isotopic reference peaks.
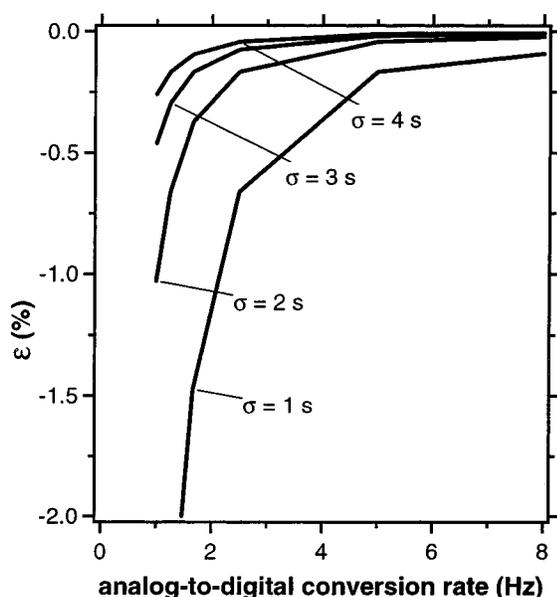


**Figure 5.** Estimated values of $\epsilon$ as a function of peak width and analog-to-digital conversion frequency. All data are for Gaussian-shaped peaks ($\sigma$ = standard deviation) with no background $H_2$ signals.



**Figure 6.** Typical relationship between δD values measured by conventional dual-inlet versus isotope ratio monitoring techniques. Least-squares regression of these data gives $y = 0.987x - 0.6$, with $r^2 = 0.9988$. The solid line is $y = x$ and is indistinguishable from the regression line at this scale.

Problems with mismatched time constants are minimized in these samples because peaks are widely separated. As a result, overall integration intervals can be significantly wider than the actual peaks. Data were collected in 250-ms integration intervals and corrected with the pointwise algorithm using values of $K$ determined from the *n*-alkane standards via the peak-rms method described by Sessions et al. (following paper). The $C_{18}$ and $C_{28}$ *n*-alkanes were chosen as isotopic reference peaks for each analysis because they are at approximately the same concentration in our standard mixture and have approximately the same δD values.

Results obtained via isotope ratio monitoring are compared to those obtained from conventional analyses in Table 3. The relationship between δD values obtained by the two methods is shown for a typical analysis in Figure 6. For all such analyses, a linear relationship was obtained with $r^2 > 0.99$ and with a slope ran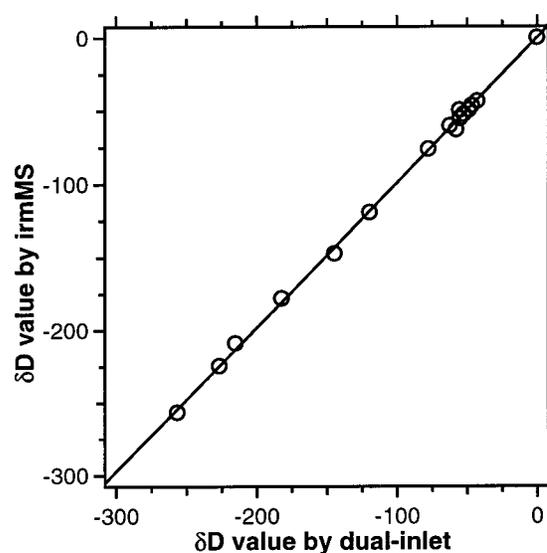ging from 0.95 to 1.02. The slope of this regression was typically reproducible to within ~0.01 when multiple samples were analyzed over the course of a day. Differences in δD values are designated by the symbol Δ in Table 3. Accuracy, expressed in terms of the rms value of Δ, is 2.5‰. Precision, expressed as the standard deviation of the population of results for each alkane ($\sigma_p$), ranges between 2.1 and 5.2‰. Systematic errors are minimized by the normalization procedure. In this case, the average value of Δ is exactly zero because the normalization is based on the alkane δD values themselves (in practical analyses, e.g., ref 2, normalizations developed from alkane test runs are applied to diverse analytes in separate chromatographic runs). In contrast, precision is unaffected by normalization, which serves only to increase or decrease the average value (i.e., Δ).

Errors in δD are uncorrelated with peak height ($r^2 = 0.002$; Figure 7). The normalization applied to these data is based only on δD value, not peak height. δD and concentration do not covary in our *n*-alkane sample mixture ($r^2 < 0.001$), so any correlation
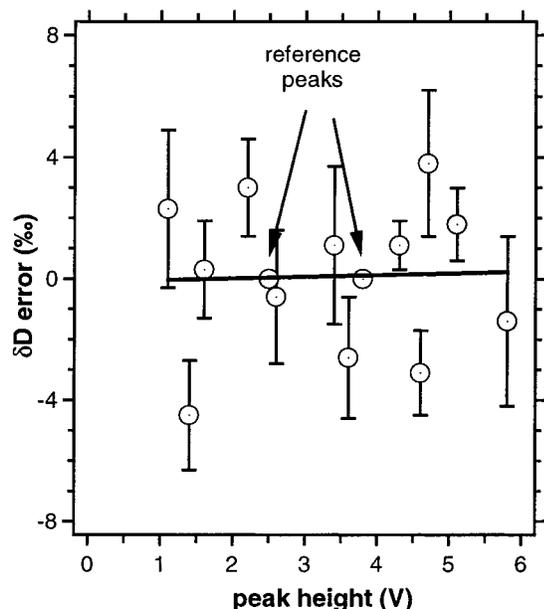
**Figure 7.** Measured errors in $\delta D$ as a function of peak height for $C_{17}-C_{30}$ n-alkanes. Error bars are $\pm 2\sigma_\Delta$ from 48 replicate analyses.

between $\Delta$ and peak height should be unaffected by normalization. To test this assertion, we calculated the correlation coefficient between peak height and errors in the $\delta D$ values obtained prior to normalization ($r^2 = 0.004$). The lack of correlation indicates no significant systematic errors are introduced by the pointwise correction of $H_3^+$. Because we have determined the value of $K$ from the chromatograms themselves, this level of accuracy and precision is probably better than can be achieved for real samples where a larger uncertainty in the value of $K$ exists. This analysis does demonstrate, however, that the pointwise algorithm can accurately accommodate GC peaks with a wide range in peak height and width, and which appear on a substantially changing $H_2$ background.

As shown in Figure 7, the scatter of the results around $\Delta = 0$ is larger than expected on the basis of the reproducibility of the $\delta D$ values. The error bars are $\pm 2\sigma_\Delta$, where $\sigma_\Delta = (\sigma_m{}^2 + \sigma_{di}{}^2)^{1/2}$ (see notes to Table 3). This range takes into account the expected random variations in the mean values of both the irmGCMS results and the dual-inlet results. Approximately 95% of the error bars would be expected to include $\Delta = 0$, but only 6 of the 12 samples do so. There is no apparent correlation between values of $\Delta$ and $\sigma_p$ for a given alkane ($r^2 = 0.08$), between $\Delta$ and carbon number ($r^2 = 0.10$), or between $\Delta$ and $\delta D$ of the alkane ($r^2 = 0.001$) or $\delta D$ of the previous alkane ($r^2 = 0.03$) as might be expected in the case of memory effects. However, the alkanes for which $\Delta$ is significantly different from zero all have $\delta D$ in the range $-50$ to $-125$‰ and are therefore likely derived from petroleum sources.[17] With one exception, the alkanes for which $\Delta$ is not significantly different from zero all have $\delta D$ in the range $-150$ to $-275$‰ and are probably derived from biological sources.[2] We suggest that the systematic errors apparent in the former group may therefore be related to the origin of these materials.

(16) Vaughn, B. H.; White, J. W. C.; Delmotte, M.; Trolier, M.; Cattani, O.; Stievenard, M. *Chem. Geol.* **1998**, *152*, 309−319.
(17) Schoell, M. *Org. Geochem.* **1984**, *6*, 645−663.

For example, minor impurities in petroleum-derived alkanes could lead to systematic differences between the compound-specific irmGCMS analyses and the bulk property conventional analyses.

As shown by Figure 2, a correlation between peak height and $\Delta$ would be expected if errors in $K$ were responsible for the scatter in the results. In more general terms, uncertainties in $K$ must propagate and lead to uncertainties in $\delta D$. The results of the sensitivity tests summarized in Figure 2 indicate that, if uncertainties in $K$ are on the order of 2% (as in this case), related errors in $\delta D$ will be on the order of a few per mil for typical sample-to-standard mismatches of peak height and $\delta D$ value. From this perspective, the rms error of 2.5‰ is not surprising. Until further experience yields a more complete understanding of factors controlling $K$, the results of the sensitivity tests reported here should—when questions of accuracy are preeminent—be given precedence over more impressive measurements of internal precision.

## CONCLUSIONS

We have shown on theoretical grounds that a correction based only on peak height can be very accurate, but only to the extent that peak shapes and background currents are constant. In typical irmMS conditions, where neither is constant, peakwise corrections can introduce large errors. The more general, pointwise algorithm avoids these problems. This method is independent of peak shape and background signals and is applicable to a wide range of hydrogen irmMS applications (including gas chromatography and elemental analysis). The accuracy of pointwise $H_3^+$ correction is limited by (1) the frequency response of the mass-2 signal-processing pathway, (2) the analog-to-digital sampling rate of the data system, and (3) the highest frequency at which $H_2$ signals change. Analog-to-digital conversion rates of at least 4 Hz and electronic time constants of <500 ms should be used to minimize $H_3^+$-related errors under typical GC conditions.

To test the proposed pointwise correction algorithm, a suite of 14 homologous n-alkanes for which concentrations vary over a 5-fold range was analyzed using our irmGCMS system. The analyses produced an rms error of 2.5‰ for means of 48 analyses. The average precision of a single measurement was 2.3‰. There is no correlation between error and peak height in these analyses, indicating that pointwise correction of $H_3^+$ does not introduce systematic errors. Assuming the "correct" value for $K$ can be determined, the correction of irmMS data for $H_3^+$ by the pointwise correction algorithm should not limit the precision of the measurements.